Available online at www.sciencedirect.com
SCIENCE DIRECT®
Materials Chemistry and Physics 97 (2006) 468–471
MATERIALS CHEMISTRY AND PHYSICS
www.elsevier.com/locate/matchemphys

The formation of perovskite $PbTiO_3$ powders by sol–gel process

Chi-Young Lee [a,b,*], Nyan-Hwa Tai [b], Hwo-Shueenn Sheu [c], Hsin-Ten Chiu [d], Shu-Hsu Hsieh [b]

[a] *Materials Science Center, National Tsing Hua University, No. 101 Sce. 2 Kung Fu Road, Hsinchu 300, Taiwan 30043, PR China*
[b] *Department of Materials Science and Engineering, National Tsing Hua University, No. 101 Sce. 2 Kung Fu Road, Hsinchu 300, Taiwan, 30043, PR China*
[c] *National Synchrotron Radiation Research Center, 101 Hsin-Ann Road, Hsinchu Science Park, Hsinchu 30077, Taiwan, PR China*
[d] *Department of Applied Chemistry, National Chiao Tung University, Hsinchu, Taiwan 30050, PR China*

Received 28 September 2004; received in revised form 8 August 2005; accepted 23 August 2005

Abstract

Nano-sized cubic $Pb_2Ti_2O_6$ and monoclinic $PbTi_3O_7$ were obtained as the first stage products, by sol–gel process using anhydrous lead acetate and titanium(IV) isopropoxide as precursors; then, as the powder was heated, $Pb_2Ti_2O_6$ gradually transformed to perovskite $PbTiO_3$ around 673 K.

Keywords: Perovskite $PbTiO_3$ powder; Sol–gel process; Pb–Ti oxides; $Pb_2Ti_2O_6$

Ferroelectric materials based on the pervoskite structure have been widely used in pyroelectric and piezoelectric devices [1]. Various preparation methods, high temperature route methods, specifically the solid-state method [2], and chemical routes [3–5], namely the MOCVD and sol–gel processes, have been explored for fabricating these materials. The solid-state method results in poor sintering behavior, a lack of homogeneity and poor control of cation stoichiometry, and is inadequate for various advanced applications. Chemical routes, particularly sol–gel processing, offer advantages over the solid-state method and have attracted strong interest. It is especially difficult to control the lead content in lead containing ceramics because of PbO volatility. Single source precursors with related stoichiometry have been used to prepare Pb–Ti oxides [6,7]. For $[PbTi_2O(OEt)_8]_m$ and $[PbTi_2O(OAc)(OEt)_7]_2$, the metal ratios did not match those of lead based ferroelectrics given $PbTi_3O_7$ and lead oxide in hydrolysis polycondensation reactions. The other compounds which have stoichiometer with material formulation, namely $Pb_2Ti_2O(OAc)_2(O^iPr)_8$, $Pb_2Ti_2O(O^iPr)_{10}$, and $Pb_2Ti_2O(acac)_2(O^iPr)_8$, may act as a single source for $PbTiO_3$. The powders resulting from the hydrolysis of $Pb_2Ti_2O(OAc)_2(O^iPr)_8$ and $Pb_2Ti_2O(acac)_2(O^iPr)_8$ lead directly to the pervoskite phase in hydrolysis, followed by calcination at 823 K. The powder resulting from $Pb_2Ti_2O(O^iPr)_{10}$ yielded a mixture of pervoskite $PbTiO_3$ and $Pb_2Ti_2O_6$. Conversion of $Pb_2Ti_2O_6$ to pervoskite occurs at 973 K. Another important observation is that the hydrolysis of $Pb_2Ti_2O(OAc)_2(O^iPr)_8$ with small amounts of water in isopropyl alcohol causes some $Pb_2Ti_2O_6$ formation. According these observations, the pervoskite $PbTiO_3$ formation might depend on the nature of the initial precursors and reaction conditions. This work examined the nature of the powders obtained by hydrolysis of the precursor solution obtained by reacting lead acetate using titanium isopropoxide under various experimental conditions, hydrolysis solution pH values, and calcinated temperatures.

Anhydrous lead acetate and titanium(IV) isopropoxide (97 wt.%, Aldrich) were used as the starting reagents for preparing PT powder. The general procedure for preparing PT powders was described as follows. The reagents, titanium(IV) isopropoxide (9.12 g, 0.04 mol) and lead acetate (13 g, 0.04 mol), were dissolved in 70 mL anhydrous ethanol and refluxed to yield a PT precursor solution. This solution then was hydrolyzed and condensed by slowly adding 70 mL aqueous solution with various pH values. Meanwhile, the solution was maintained at 353 K under stirring. A white precipitate appeared and the clear solution turned to turbid sols with addition of aqueous solution. Following the completion of aqueous solution addition, the sols were heated for 8 h to complete the hydrolysis and condensation. Afterward hydrolysis and drying at 423 K, a white powder containing lead, titanium and oxygen, as suggested by EDS (energy dispersive spectroscopy), was isolated with a nearly quantitative

* Corresponding author. Tel.: +88 635 728692; fax: +88 635 166687.
E-mail address: cyclee@mx.nthu.edu.tw (C.-Y. Lee).

0254-0584/$ – see front matter © 2005 Elsevier B.V. All rights reserved.
doi:10.1016/j.matchemphys.2005.08.048

yield. The white powder then was calcinated at 673–973 K for 4 h.

The surface morphologies of the powders were examined using a LEO 1530 field emission scanning electron microscope (FESEM) fitted with an energy dispersive X-ray spectrometry system (EDS) for element detection. Moreover, crystallinity and morphological analysis of the powders was performed using a Phillips Tecnai 20 transmission electron microscope (TEM). The phase detection and analysis of the powders was performed using a MAC SCIENCE MXP-3 type diffractometer (XRD) with Cu Kα radiation.

Fig. 1 illustrates images and their corresponding electron diffraction patterns of the white powder without calcination. The nanoparticles were extremely uniform, with a diameter of ∼3 nm. The electron diffraction patterns of nanoparticles comprised relatively blurred rings that can be indexed as (2 2 2), (4 0 0), (4 4 0) and (6 2 2) of cubic $Pb_2Ti_2O_6$. High-resolution TEM (HRTEM) images of the as prepared powder demonstrated each particle as being single crystal with a diameter of several nanometers.

Fig. 2 shows the TEM image and ED of the powder calcinated at 973 K. Fig. 2(a) indicates that the particles have a diameter of ∼100 nm, exceeding that of the particles without calcination. Additionally, the electron diffraction patterns of particles comprised clearly concentric circles that can be indexed as (1 0 0), (1 0 1), (1 1 1), (1 0 2), (2 1 1) and (2 0 2) of tetragonal perovskite $PbTiO_3$.

The microstructures of the powders hydrolyzed and then calcinated at various temperatures were further studied via XRD measurement. These results demonstrated that the powders calcined below 723 K were primarily amorphous in structure, as shown by the broad weak signals in the XRD patterns in Fig. 3.

Observations of phase evolution clearly reveal the coexistence of $PbTi_3O_7$ and a tetragonal perovskite phase for the powders obtained by hydrolysis and calcinated at 773 K. Further increasing the calcination temperature gradually eliminates the $PbTi_3O_7$ phase and increases the perovskite phase. The complete transformation of the $PbTi_3O_7$ phase to the tetragonal perovskite phase appears to occur at 873 and 973 K for the powders obtained by hydrolysis in the solutions with the pH 3 and 7, respectively. However, the phase evolution for the powder obtained via hydrolysis in the solution with pH 12 displayed that a perovskite structure with a pure tetragonal phase of $PbTiO_3$ could directly obtained at 773 K, and no diffraction peaks because of any other phases appeared during the evolution.

This investigation also attempted to determine the average size of the crystalline particles by using diffraction line broadening of XRD. Using Scherrer's equation, the average crystal size of the particle was calculated from the (1 0 1) reflection as being 29 nm for the powder calcinated at 773 K, and 43 nm for

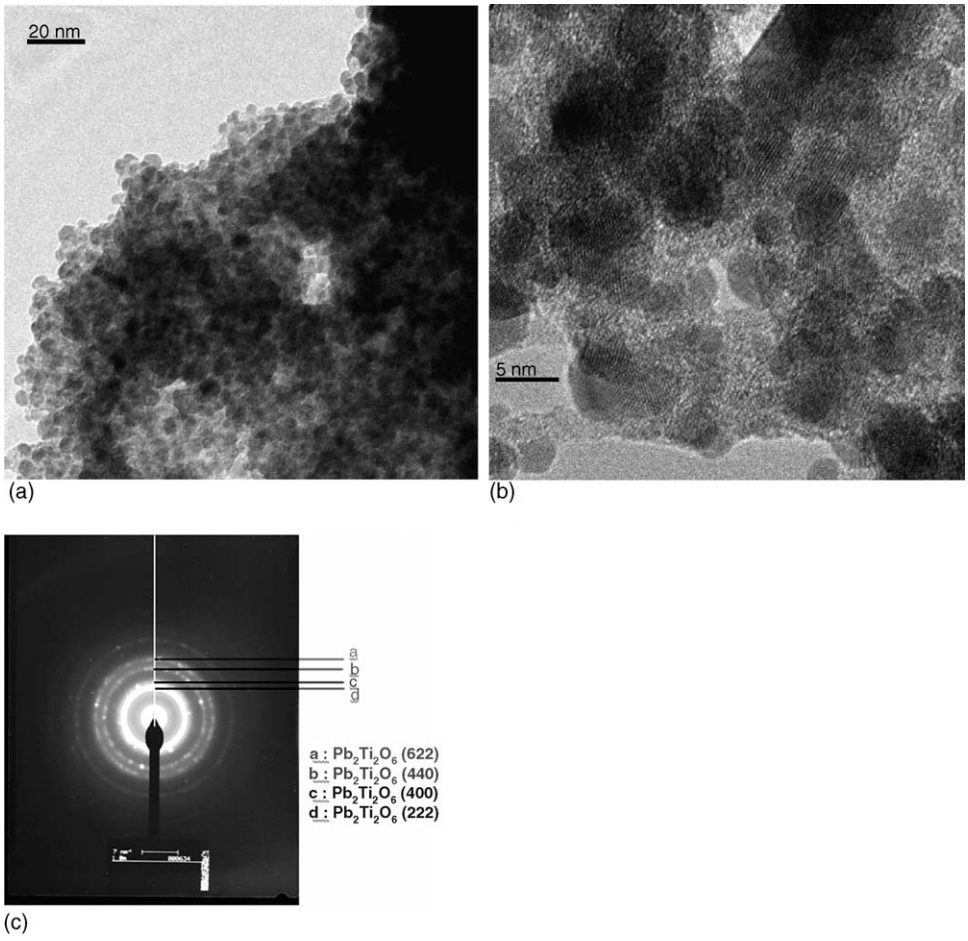

Fig. 1. TEM images and corresponding electron diffraction patterns of the as prepared white powder.

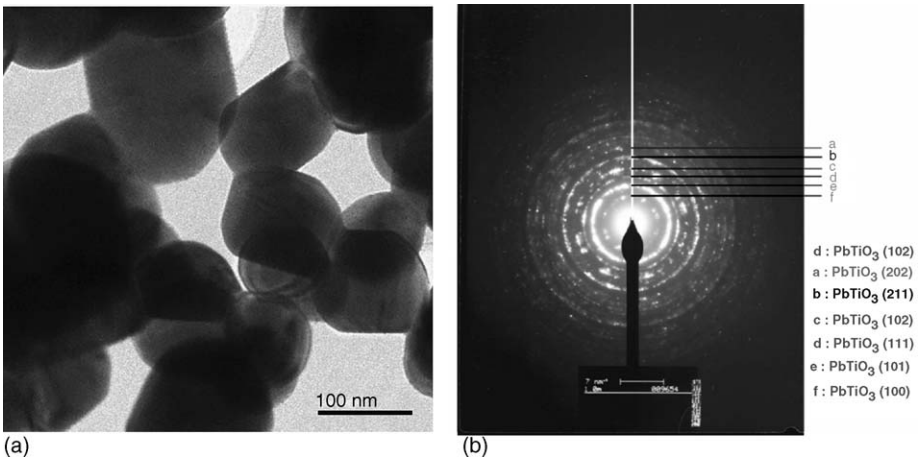

Fig. 2. TEM images and corresponding electron diffraction patterns of the powder calcinated at 973 K.

the powder calcinated at 973 K. The size of the obtained particles increased with the calcinations temperature. On the other hand, XRD diffraction peak of the powder calcinated below 773 K was broad and had low intensity. This phenomenon suggests that the crystal size of the particles was very small or the powder was amorphous. Furthermore, the structures of the powder without calcination were characterized by high resolution XRD using a synchrotron radiation 20 KeV X-ray.

The grain size is approximately 1.5 nm ± 1 nm, as calculated according to the FWHM of the X-ray powder diffraction pattern using the Scherrer equation. Rietveld refinement [8,9] was used to characterize the non-calcinated sample that used two phases of $Pb_2Ti_2O_6$ (major) and $PbTi_3O_7$ (minor), as illustrated in Fig. 4. $Pb_2Ti_2O_6$ was first introduced to fit XRD data following the addition of converged phase two ($PbTi_3O_7$). The crystal parameters of $PbTi_3O_7$, include cell dimensions, atomic coordinates and thermal parameters, are described in the literature [10]. The final Rietveld refinement was converged to the $R_p = 1.26\%$, $wR_p = 1.70\%$, $\chi^2 = 10.8\%$ and cell dimension $a = 10.4477$ (8) Å of $Pb_2Ti_2O_6$.

Fig. 5 shows SEM images of the powders hydrolyzed and then calcinated at various temperatures. The image of the non-calcinated powder (Fig. 5(a)) displayed that the powders contain some large particles and agglomerates surrounded by smaller particles. The sizes of the agglomerates are 10–20 nm. The mean particle diameter increased with calcination temperature. At temperature of 973 K, the average grain sizes are approximately 100 nm, as illustrated in Fig. 5(c).

The SEM images reveal that the powder grain size evolved with increasing calcination temperature. Significant differences could be observed for the powders calcinated at 723 K compared with their as-prepared state. Coarsening is apparent in Fig. 5(b). The nanoscale particles are believed to have coalesced into larger particles with any grain boundary elimination.

Large particles with smooth surfaces are noted as the calcinated temperature increased from 723 to 973 K. This observation implies that the particles merge together in the calcination process. For powders heated at 973 K, coalescence and growth of the primary particles becomes more evident, causing a significant increasing average grain size, as illustrated in Fig. 5(b) and (c). It appears that several small particles merged to form a single larger particle.

The DSC profile displays a broad exothermic peak corresponding to the elimination of the absorption moisture on the

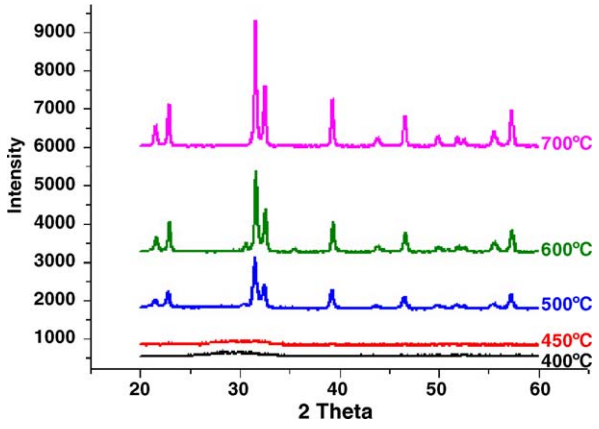

Fig. 3. XRD patterns of the powders calcinated at various temperatures.

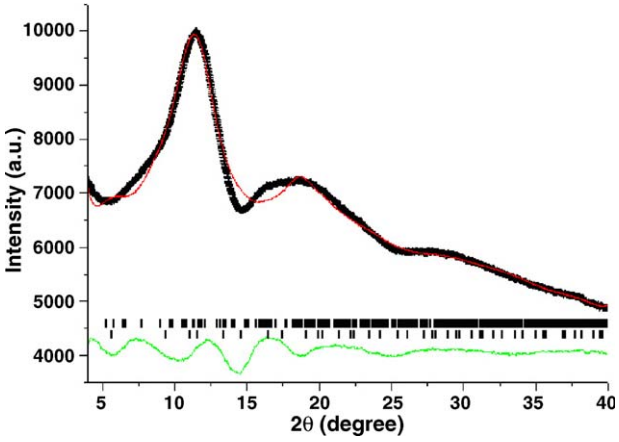

Fig. 4. Rietveld refinement using two phases of $Pb_2Ti_2O_6$ (major) and $PbTi_3O_7$ (minor); (+) denotes the experimental data; solid line, the simulation curve; short bar, the reflection positions; green curve, different intensity of experimental data and simulation data.

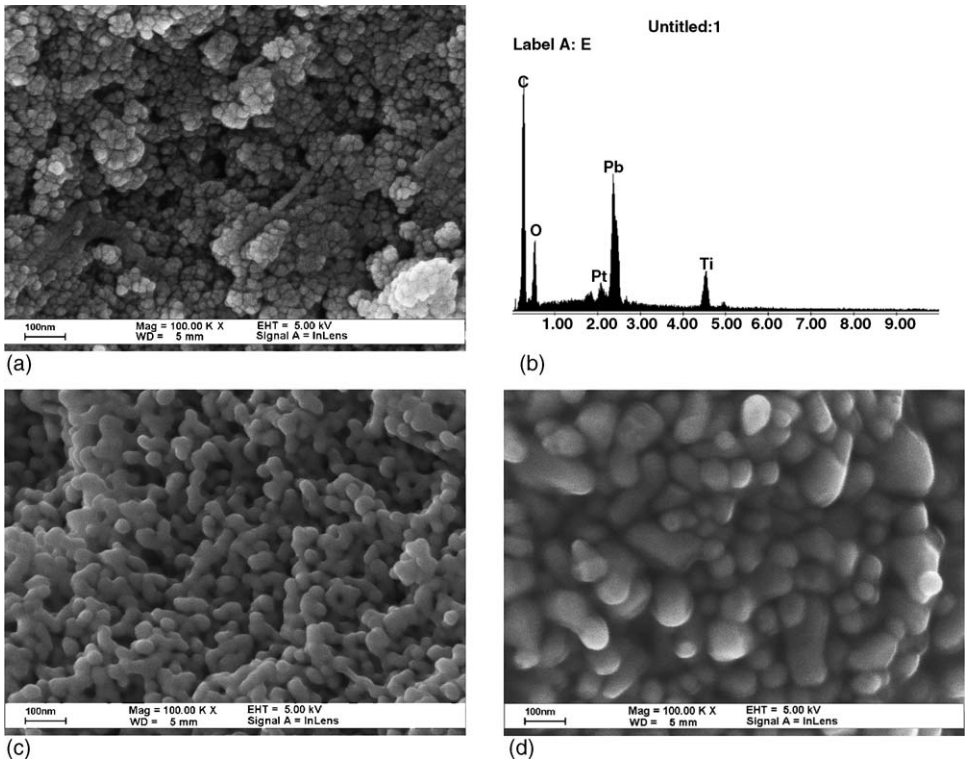

Fig. 5. SEM images and corresponding EDS of the powder calcinated at various temperatures; (a) as prepared powder; (b) EDS of the as prepared powder; (c) calcinated at 723 K; (d) calcinated at 973 K.

powder surface near 373 K, while a broad endothermic peak indicating crystallization and grain growth is noted towards 623 K. This result consists with the SEM observation.

This investigation has explored the formation of sol–gel process of $PbTiO_3$ powers. Anhydrous lead acetate and titanium(IV) isopropoxide were used as starting reagents for preparing $PbTiO_3$ powder. The $PbTiO_3$ powders obtained generally have fine particle and narrow particle size distribution. The grain size of the as-prepared particles is approximately $1.5\,nm \pm 1\,nm$ calculated using the FWHM of the X-ray powder diffraction pattern by Scherrer equation and TEM images. According to Rietveld refinement and electron diffraction, the non-calcinated sample comprised two phases, the major phase is cubic $Pb_2Ti_2O_6$ and the minor phase is $PbTi_3O_7$. Then, during heat treatment, $Pb_2Ti_2O_6$ gradually transformed to perovskite $PbTiO_3$ near 673 K. Furthermore, the obtaining of crystalline $Pb_2Ti_2O_6$ in the as-prepared state was not influenced by the pH value in the hydrolysis condition. This is the first time perovskite $PbTiO_3$ powders formation process be studied.

References

[1] J. Moon, J.A. Kerchner, J. LeBleu, A.A. Morrone, J.H. Adair, J. Am. Ceram. Soc. 80 (10) (1997) 2613.
[2] S.S. Cole, H. Espenschied, J. Phys. Chem. 41 (1937) 445.
[3] S.R. Gurkovich, J.B. Blum, in: L.L. Hench, D.R. Ulrich (Eds.), Ultrastructure Processing of Ceramics, Glasses and Composites, John Wiley and Sons, New York, 1984.
[4] S.R. Gurkovich, J.B. Blum, Ferroelectrics 62 (1985) 189.
[5] J.B. Blum, S.R. Gurkovich, J. Mater. Sci. 20 (1985) 4479.
[6] S. Daniele, R. Papiernik, L.G. Hubert-Pfalzgraf, S. Jagner, M. Hikansson, Inorg. Chem. 34 (1995) 628.
[7] L.G. Hubert-Pfalzgraf, S. Daniele, R. Papiernik, M.C. Massiani, B. Septe, J. Mater. Chem. 7 (5) (1997) 753.
[8] H.M. Rietveld, J. Appl. Cryst. 2 (1969) 65.
[9] A.C. Larson, R.B. von Dreele, Generalized Structure Analysis System, Los Alamos National Laboratory, Los Alamos, NM, 1994.
[10] K. Kato, I. Kawada, K. Muramatsu, Acta Cryst. B24 (1982) 1968.